Applied Catalysis B: Environmental 111–112 (2012) 218–224

Contents lists available at SciVerse ScienceDirect

Applied Catalysis B: Environmental

journal homepage: www.elsevier.com/locate/apcatb

Catalytic performance of core–shell and alloy Pd–Au nanoparticles for total oxidation of VOC: The effect of metal deposition

M. Hosseini[a,b,*], T. Barakat[a], R. Cousin[a], A. Aboukaïs[a], B.-L. Su[c], G. De Weireld[d], S. Siffert[a,*]

[a] Unité de Chimie Environnementale et Interactions sur le Vivant (UCEIV), Université Lille Nord de France, ULCO, E.A. 4492, F-59140 Dunkerque, France
[b] Department of Chemistry, University of Texas at El Paso, 500 W. University Ave., El Paso, TX 79968-0513, USA
[c] Laboratoire de Chimie des Matériaux Inorganiques, Facultés Universitaires Notre Dame de la Paix, 61 rue de Bruxelles, 5000 Namur, Belgium
[d] Laboratoire de Thermodynamique Physique-Mathématique, Université de Mons, 31 boulevard Dolez, 7000 Mons, Belgium

ARTICLE INFO

Article history:
Received 14 May 2011
Received in revised form
28 September 2011
Accepted 4 October 2011
Available online 10 October 2011

Keywords:
VOC oxidation
Palladium
Gold
Mesoporous TiO_2
Core–shell
Alloy
UV–vis diffraction
Operando DRIFT
TPR

ABSTRACT

The catalytic properties of palladium and gold nanoparticles deposited on mesoporous TiO_2 are investigated in toluene and propene oxidation. The catalysts, containing Pd and Au deposited on mesoporous TiO_2 have been prepared by different order of metal deposition (Pd(shell)–Au(core)/TiO_2, Pd–Au(alloy)/TiO_2 and Au(shell)–Pd(core)/TiO_2. For both toluene and propene oxidation reactions, the catalytic activity was found significantly higher when palladium is deposited on already-deposited gold (Pd(shell)–Au(core)/TiO_2). This enhanced activity could be explained by the core–shell morphology (Pd–shell and Au-core) observed by UV–vis spectra, TPR profiles and XPS spectra. It was suggested that the oxidation reaction follows a Langmuir–Hinshelwood mechanism where the molecules of oxygen and VOC are in competition for adsorption on the surface of catalyst. Operando DRIFT spectroscopy was carried out to test the catalytic activity in a mixture of volatile organic compounds (toluene and propene). It was demonstrated that there is a competition between the molecules of VOC for adsorption but also the toluene has an inhibition effect for oxidation of propene.

1. Introduction

Volatile organic compounds (VOCs) are the common air pollutants emitted by motor vehicles as well as the chemical and petrochemical industries. Control of VOCs emission is a major concern of the industries' commitment towards the environment and human health. In recent years, many studies have been focused on the catalytic oxidation of VOCs [1–3]. A catalytic system combusts these compounds at temperatures lower than those of thermal oxidation (about 300–400 °C) [4]. This system that reduces the combustion energy requirements is well suited to low VOC concentration range (100–2000 ppm).

Many studies have revealed the high catalytic activity of Noble metals (Pd, Pt, Ru, Au, etc.) supported on different oxides in a number of oxidation reactions [5–8]. It has also been reported that it is possible to modify the monometallic catalyst by adding a second metal to improve the dispersion, adsorption and activity towards the oxidation of hydrocarbons [9]. Another effective method of enhancing catalytic activity is the core–shell construction of nanosized bimetallic particles [10]. The Au–Pd is one of the core–shell systems that have gained considerable attention [11,12]. Several investigations show that depending on the preparation method and treatment, particles with a homogeneous alloy [13,14] and core–shell morphology [10,15] have been identified. The catalytic performance could change with the different structural properties and electronic configuration of core–shell and alloy nanoparticles [16,17]. Other studies show that catalytic properties of bimetallic nanoparticles are correlated to the difference between the adsorption of the molecules of reactive on core–shell and alloy structure [18,19].

In an earlier paper concerning the synthesis of Pd–Au, we showed that catalysts based on core–shell Au–Pd supported on titania can provide a significantly improved activity in the oxidation

* Corresponding authors at: Unité de Chimie Environnementale et Interactions sur le Vivant (UCEIV), Université Lille Nord de France, ULCO, E.A. 4492, F-59140 Dunkerque, France. Tel.: +33 328658256.
E-mail addresses: mhosseini@utep.edu (M. Hosseini), siffert@univ-littoral.fr (S. Siffert).

0926-3373/$ – see front matter © 2011 Elsevier B.V. All rights reserved.
doi:10.1016/j.apcatb.2011.10.002

reaction of VOCs compared with the Au-pure and Pd-pure catalysts [20]. In this study, we extend our initial results and report a detailed investigation of core–shell and also alloy Au–Pd catalysts supported on mesoporous TiO_2. This support was chosen because it was considered as one of the most promising supports for the total oxidation of VOCs, especially after depositing Pd [21,22] and gold [23,24], also due to its stability and high surface area [25].

2. Experimental

2.1. Preparation of catalyst

Mesoporous TiO_2 was used as support essentially for its high surface area. It was prepared by $Ti(OC_2H_5)_2$ in the presence of surfactant CTMABr as described elsewhere [26].

Two monometallic Pd/TiO_2 and Au/TiO_2 and three bimetallic catalysts Pd(shell)–Au(core)/TiO_2, Au(shell)–Pd(core)/TiO_2 and Pd–Au(alloy)/TiO_2 have been synthesized.

The samples, Pd(shell)–Au(core)/TiO_2 and Au(shell)–Pd(core)/TiO_2 were prepared by the different deposition order of Pd and Au.

In the case of sample Pd(shell)–Au(core)/TiO_2, 0.5 wt% Pd was deposited onto the surface of previously prepared 1% Au/TiO_2, where for the sample Au(shell)–Pd(core)/TiO_2, 1 wt% of gold was added to previously prepared 0.5%Pd/TiO_2 [27].

1 wt% of gold was deposited through a chemical interaction of $HAuCl_4{\cdot}3H_2O$ and Na_2CO_3 in aqueous solution, under complete control of all parameters, temperature, pH, stirrer speed, using deposition-precipitation method. The precipitation was performed for 4 h at 80 °C, filtered and washed until an absence of Cl^- ions. Then, the deposited samples were dried at 80 °C over night.

0.5 wt% of palladium was introduced via impregnation with aqueous solution of $PdNO_3$ for 2 h and samples were dried at 60 °C in rotary evaporator. All the samples were calcined in air at 400 °C for 4 h after each metal deposition.

The third sample Pd–Au(alloy)/TiO_2, was prepared by adding the aqueous solution of $PdNO_3$ and $HAuCl_4$ to the colloid of support (mesoporous TiO_2) at the same time. This deposition was performed using deposition-precipitation method. After filtering, washing and drying, the sample was calcined under air at 400 °C for 4 h.

Through these techniques, we prepared three different catalysts. For the first two techniques, only core–shell catalysts should be obtained according to the work of Hutchings and co-workers [28–31].

2.2. Catalyst characterization

The catalyst specific surface areas were measured by N_2 adsorption–desorption at −196 °C with a volumetric adsorption analyzer Sorptomatic 1990 manufactured by Thermo Finnigan. Prior to measurement, samples were out gassed at 120 °C.

Elemental analysis of the catalysts was performed in analytical center of France CNRS (Vernaison) by using an inductively couples plasma optical emission spectroscopy and mass spectroscopy (ICP/OES/MS) after dissolution of sample on a mixture of HF and HNO_3 solution.

UV–vis diffuse reflectance (UV-vis-DR) spectra were recorded with a Cary 5000 Scan (Varian) spectrophotometer in the spectral range of 200–800 nm.

The X-ray diffraction (XRD) pattern was recorded in a D8 Advanced Bruker AXS diffractometer with a Cu Kα radiation (l = 1.5406 Å). Diffraction patterns were recorded over a 2θ range from 20° to 80°.

Table 1
BET surface area, elemental analysis (gold and palladium content) of solids.

Samples	BET surface area ($m^2\,g^{-1}$)	Metal (wt%)	
		Pd	Au
Pd/TiO_2	173	0.46	–
Au/TiO_2	153	–	0.96
Pd(shell)–Au(core)/TiO_2	151	0.39	0.80
Au(shell)–Pd(core)/TiO_2	127	0.37	0.79
Pd–Au(alloy)/TiO_2	149	0.37	0.81

The temperature programmed reduction (TPR) profiles were recorded using an Altamira AMI-200 apparatus. Samples (100 mg) were heated from −40 up to 500 °C at a heating rate of 5 °C min^{-1} in a flow of 5% H_2/Ar (30 mL min^{-1}) and hydrogen consumption was monitored and integrated using thermal conductivity (TC) detection over the whole temperature range.

The X-ray photoelectron spectroscopy (XPS) analysis was performed using a Perkin-Elmer ESCA Phi 560 system with Mg Kα radiation. XPS spectra were acquired after ultrahigh vacuum (UHV) recovery and stabilization below 10^{-8} torr. These last experiments were obtained in the University of Texas at El Paso.

2.3. Catalytic activity

The catalytic activity of 100 mg impregnated catalyst was examined by measuring the conversion of 1000 ppm toluene and 3000 ppm of propene in air. The oxidation reaction was carried out in a fixed bed microreactor between 25 and 400 °C (1 °C min^{-1}) under 100 mL min^{-1} flow of gas mixture (air + toluene and air + propene). Prior the oxidation reaction, the catalyst were calcined under a flow of air (2 L h^{-1}) at 400 °C (1 °C min^{-1}) and then reduced under hydrogen flow (2 L h^{-1}) at 200 °C (1 °C min^{-1}).

The catalytic test for oxidation of a mixture of toluene and propene has been carried out and followed by Operando Diffuse Reflectance Infrared Fourier Transform (DRIFT) spectroscopy in the same condition as described above for the normal test. The Operando DRIFT spectroscopy was performed in the 1000 and 4000 cm^{-1} range using an Equinox 55 Bruker spectrometer equipped with a liquid nitrogen cooled mercury–cadmium–telluride (MCT) detector.

3. Results and discussion

Table 1 presents the BET specific surface areas measured after calcinations at 400 °C and the elemental analysis of the mono and bimetallic samples. All solids show a high specific surface area with the amount of metals close to those expected and equivalent for the three samples (0.4 wt% Pd and 0.8 wt% Au). The results demonstrate that the sample Pd(shell)–Au(core)/TiO_2, with the deposition of Pd on gold particles has a higher specific surface area. The addition of gold on the palladium resulted in reduce of the surface area (173 to 127 $cm^2\,g^{-1}$) while the sample Au/TiO_2 was not really affected by deposition of palladium (153 to 151 $cm^2\,g^{-1}$). The solid Pd–Au(alloy)/TiO_2 shows a surface area close to Pd(shell)–Au(core)/TiO_2.

All synthesized samples present the anatase phase with a low part of brookite phase for the mesoporous TiO_2, as determined by X-ray powder diffractometry (graph not shown). The metallic gold and/or palladium or their oxides were not detected by XRD experiment. This could be due to the fact that (i) noble metal content of our samples is low and that (ii) Pd and/or Au particles are well-dispersed onto the support These are the main two reasons behind the absence of noble metals specific XRD peaks.

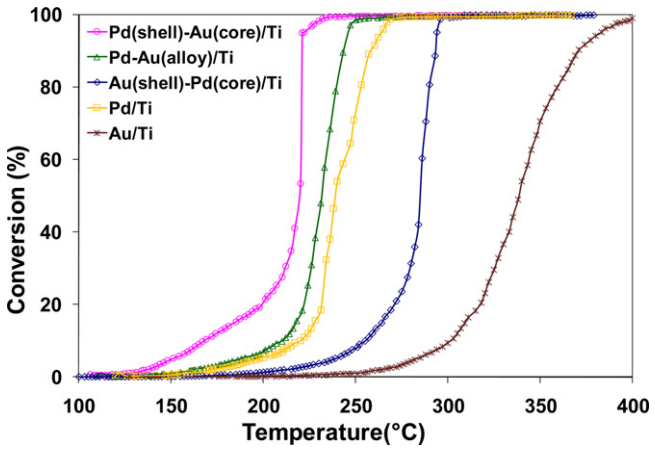

Fig. 1. Conversion of toluene on Pd(shell)–Au(core)/TiO_2, Au(shell)–Pd(core)/TiO_2, Pd–Au(alloy)/TiO_2, Pd/TiO_2 and Au/TiO_2.

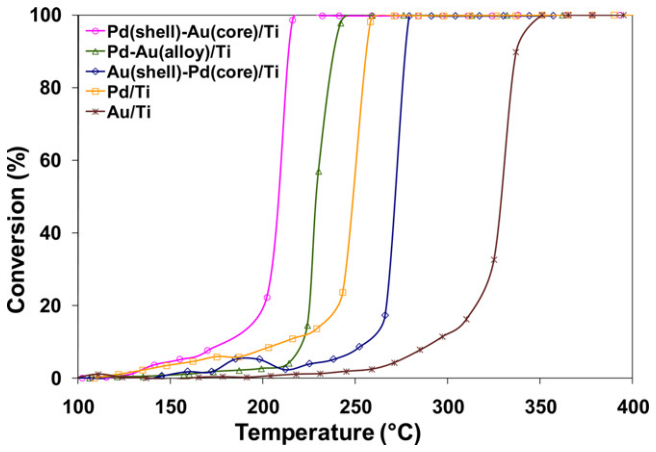

Fig. 2. Conversion of propene on Pd(shell)–Au(core)/TiO_2, Au(shell)–Pd(core)/TiO_2, Pd–Au(alloy)/TiO_2, Pd/TiO_2 and Au/TiO_2.

Figs. 1 and 2 show the conversion of toluene and propene, respectively, as a function of the reaction temperature for Pd/TiO_2, Au/TiO_2, Pd(shell)–Au(core)/TiO_2, Au(shell)–Pd(core)/TiO_2 and Pd–Au(alloy)/TiO_2 catalysts.

Bimetallic Pd(core)Au(shell)/TiO_2 and Pd–Au(alloy)/TiO_2 show a higher activity than Pd/TiO_2, where the Au(shell)–Pd(core)/TiO_2 sample has a lower activity than pure Pd. In the case of Pd(core)Au(shell)/TiO_2, Enache et al. [30] and Corma and co-workers [32–34] stated that Au–H and Pd–H species are formed in the oxidation of benzyl alcohol onto bimetallic systems. They stated that these species play an important role in the oxidation of these products and the formation of toluene. Enache et al. [31] also confirmed through another work that in Pd(shell) Au (core) systems, gold acts as an electronic promoter for Pd, all of which should explain the better activity for Pd(shell)Au(core)/TiO_2 catalyst. However, the catalytic activity for both toluene and propene total oxidation, was significantly higher with the Pd(shell)–Au(core) structure, schematized in Fig. 3a.

The oxidation reaction curves affirm that the catalytic activity of all three bimetallic catalysts depends on the latters' surface structure and is obviously related to the order of deposition of metals. For Pd(shell)–Au(core)/TiO_2 and Au(shell)–Pd(core)/TiO_2 samples, a three-layer morphology consisting of support, first deposited metal-core and second deposited metal–shell are formed (Fig. 3a and b). In the case of Pd–Au(alloy)/TiO_2 a random structure containing an alloy of Pd and Au is proposed (Fig. 3c). It should be noted that Fig. 3 schemes are illustrations used only to describe the differences between these three morphologies and are not based on characterization tests.

The formation of Pd(shell)–Au(core) structure has been reported previously in the preparation of bimetallic nanoparticles [35]. Takatani et al. [36] also found that Pd(shell)–Au(core) particles were more active for the selective partial hydrogenation than a random mixture of Pd and Au. Interestingly, the sample with Pd(shell)–Au(core)/TiO_2 reported in our study was found to be the most active and the catalyst Pd–Au(alloy)/TiO_2 was more active than Au(shell)/Pd(core)/TiO_2. Idakiev et al. [37] have found a similar core–shell effect for gold–vanadium catalysts deposited on mesoporous TiO_2 and ZrO_2 in oxidation of benzene. The authors reported that for both series of the supports the high activity was observed when the gold was the first loaded metal.

UV–vis spectroscopy and temperature programmed reduction were used to confirm the existence of the layer of Au over Pd particles for Au(shell)–Pd(core)/TiO_2.

The UV–vis spectra for Pd(shell)–Au(core), Au(shell)/Pd(core) and Pd–Au(alloy)/TiO_2 are presented in Fig. 4. The spectral zone between 200 and 350 nm corresponds to the electron transition of Ti^{4+} and a ligand of oxygen [38]. These are characteristics of anatase phase [39]. The spectrum of Pd(shell)–Au(core)/TiO_2 shows a broad band around 560 nm with a shoulder at 622 nm. In the literature [40,41], the peak observed around 550 nm was attributed to the surface plasmon resonance (SPR) of spherical nanoparticles of metallic gold. In some studies after observation by transmission electron microscopy, it was reported that the split of the SPR absorption into two bands corresponds to the oscillation of the free electrons along and perpendicular to the long axis of the rod-shaped gold nanoparticles [42,43]. However, in our samples, no rod-shaped particles were observed by TEM, on the contrary, TEM pictures show clearly the existence of spherical particles of gold loaded onto TiO_2 support [20]. Moreover, since this resonance is on the interface of the metal and the external medium (air or metal oxide for example), these oscillations are very sensitive to metal–external medium interaction. As the gold deposited on the support does not form only a monolayer of atoms, there exist not only an interface between atoms of gold and support (atoms of edge), but also a free surface of the particles being in contact with air (atoms of surface) (Fig. 5).

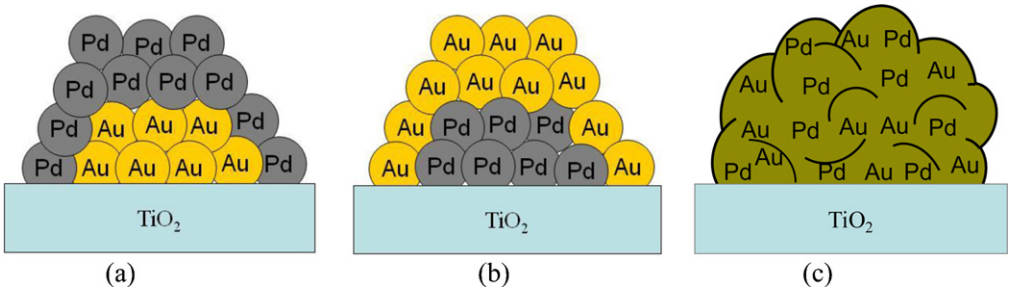

Fig. 3. Models proposed for: (a) Pd(shell)–Au(core)/TiO_2, (b) Au(shell)–Pd(core)/TiO_2 and (c) Pd–Au(alloy)/TiO_2.

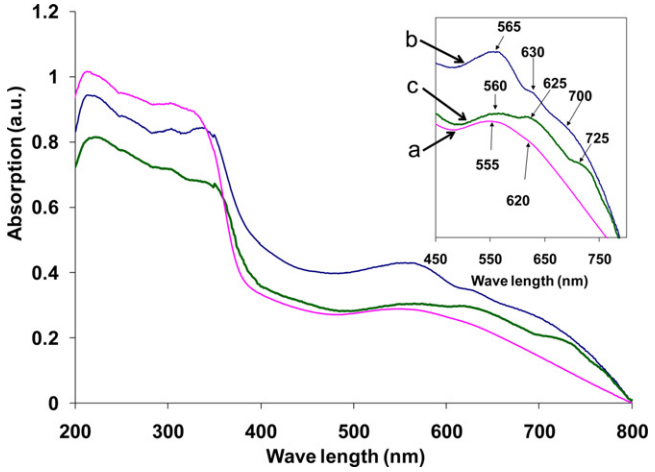

Fig. 4. DR-UV-vis spectra of: (a) Pd(shell)–Au(core)/TiO_2, (b) Pd–Au(alloy)/TiO_2 and (c) Au(shell)–Pd(core)/TiO_2.

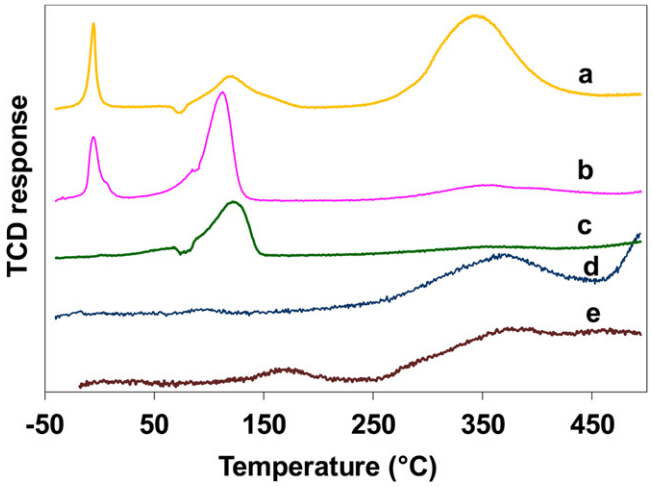

Fig. 6. H_2-TPR profile of calcined catalysts: (a) Pd/TiO_2, (b) Pd(shell)–Au(core)/TiO_2, (c) Pd–Au(alloy)/TiO_2, (d) Au(shell)–Pd(core)/TiO_2, (e) Au/TiO_2.

In this case, the first band around 560 nm could be attributed to the resonance of the atoms of surface in interaction with air and the second band around 630 nm could correspond to the atoms of edge that are in strong interaction with the support.

The same behavior was observed for the catalyst Au(shell)/Pd(core)/TiO_2 and Pd–Au(alloy)/TiO_2 with an additional shoulder at around 700 and 720 nm, respectively. This one could correspond to the atoms of gold that are in interaction with atoms of palladium.

The decrease in the intensity of peaks in Pd(shell)–Au(core)/TiO_2 compared to those of Au(shell)–Pd(core)/TiO_2, could be explained by the development of a core–shell structure for the metal particles on the catalyst. The absorbance of gold atoms in the core was then attenuated due to the presence of Pd shell. For the Pd(shell)–Au(core)/TiO_2 a layer of Pd over the previously deposited Au, is considered. The inverse position is then suggested for Au(shell)–Pd(core)/TiO_2.

Temperature programmed reduction profile for Pd–Au and Au–Pd/TiO_2 (Fig. 6) confirm the results obtained by UV–vis spectra. Since the catalysts have been in contact with air and their oxidation was limited to the surface, an oxide layer should have chemisorbed on the surface of the metal. The positive peaks observed in these profiles are then assigned to the reduction of metal oxides. The TPR profiles for Pd/TiO_2 and Pd(shell)–Au(core)/TiO_2 show two strong peaks at around −10 and 150 °C and a broad peak around 300 °C. Previously we reported that the first peak of hydrogen consumption around −10 °C is attributed to the reduction of small particles of palladium oxide located on the surface of catalyst [26]. The second positive peak (∼150 °C) also could correspond to the reduction of large particles of palladium oxide or those within the pores. The integration of two first peaks in these samples shows that the experimental hydrogen consumption value for reduction of palladium oxide (166 μmol g^{-1}) is higher than those of theoretical (69 μmol g^{-1}). Therefore, this is possible that the second peak

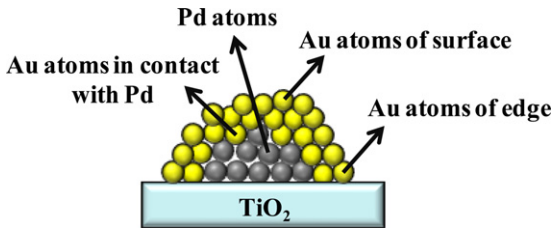

Fig. 5. Model for the core–shell morphology of Au(shell)–Pd(core)/TiO_2.

assigned either to the reduction of some part of mesoporous TiO_2 in interaction with noble metal. Moreover, the first intense positive peak of palladium oxide was not observed for Pd–Au(alloy)/TiO_2 compared to Pd(shell)–Au(core)/TiO_2 TPR profile. This is mainly due to the change in the chemistry of palladium when the latter is present in an alloy (Pd–Au). The reduction of Ti^{4+} at lower temperature in the presence of Pd has been also reported by Li et al. [44]. This early reduction could be explained by the diffusion of adsorbed and dissociated hydrogen on the palladium to the TiO_2 which results in reduction of Ti^{4+} to Ti^{3+}. The third broad peak is then attributed to the reduction of support. The TPR profile of Au(shell)–Pd(core)/TiO_2 (d) shows very small peaks below 150 °C corresponding to the reduction of palladium oxide. The weakness of these peaks indicates that the particles of palladium are covered by gold and are not accessible. It should be noted that the gold particles are stable under oxidation and reduction treatment and no peak corresponding to the reduction of these species is observed. In the case of Pd–Au(alloy)/TiO_2, a very weak peak was observed at low temperatures and a broad peak at around 150 °C. These peaks attributed to the reduction of palladium, are attenuated because of less accessibility of palladium in this sample due to the random position of palladium in the particle. In general, these TPR profiles show the existence of core–shell and alloy morphology for our samples.

The surface properties and the chemical states of the two metals were investigated by X-ray photoelectron spectroscopy. The experimental spectra are shown in Fig. 7 for bimetallic samples.

The Pd 3d spectra of the Pd(shell)–Au(core)/TiO_2 sample (a), characterized by the two spin-orbit components Pd $3d_{5/2}$ and Pd $3d_{3/2}$ separated by 5.5 eV, exhibit two doublets indicating that Pd is in highly ionic Pd^{2+} state [45]. For the sample Au(shell)–Pd(core)/TiO_2 (b) and Pd–Au(alloy)/TiO_2 (c), the peak appeared at 335.5 eV is attributed to the presence of Au $4d_{5/2}$, in agreement with literature data [29]. Gold binding energy is typical of metallic state [46,47]. The lower intensity of this peak in the case of Pd–Au(alloy) is due to the random position of gold and less availability of gold on the surface compared to Au(shell)–Pd(core).

However, the origin of the higher catalytic activity of Pd(shell)–Au(core)/TiO_2 is not really clear. It could arise from a number of possibilities, including higher adsorption of oxygen due to: (a) lower ability of Au to polarize oxygen bound than those of Pd; and (b) higher binding energy O–Pd(shell)–Au(core) than those for O–Au(shell)–Pd(core). In fact, the reaction follows the Langmuir–Hinshelwood mechanism, in which there is a

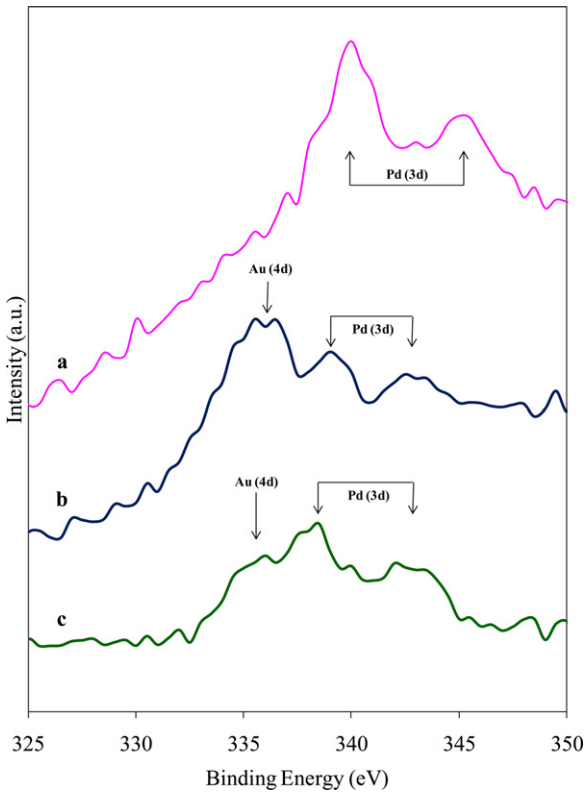

Fig. 7. XPS spectra of (a) Pd(shell)–Au(core)/TiO_2, (b) Au(shell)–Pd(core)/TiO_2 and (c) Pd–Au(alloy)/TiO_2.

competition between oxygen and VOC molecules for adsorption. Oxygen adsorbs first on the surface and then partially oxidizes the metallic surface and forms a complex which interacts with the adsorb VOC molecule. In the mixture of toluene and propene, the oxidation reaction follows the same mechanism in which oxygen molecules adsorb in the first step and then there is a preferential adsorption of toluene.

The lower activity of Au(shell)–Pd(core)/TiO_2 could be either related to the lower affinity of this solid for adsorption of oxygen due to the lower ability of Au to polarize oxygen molecule. Although certain authors reported that gold did not chemisorb oxygen [48], but Kul'kova and Levchenko [49] found that oxygen chemisorption takes place in the temperature range 50–400 °C. Berndt et al. [50] also reported a dissociative oxygen adsorption on gold. It has been also reported that adsorption of oxygen on the metal needs a spin polarization provided by metal [51]. The low adsorption of oxygen on gold may be related to the high stability of gold and lower ability to polarize the O=O bond.

According to our previous study on adsorption of the VOC molecules over noble metal [26] we suggest a Langmuir–Hinshelwood mechanism for oxidation reaction in which there is a competition for adsorption between molecular oxygen and VOC molecules. In the case of Pd(shell)–Au(core)/TiO_2 the adsorption of oxygen causes the formation of a [Pd–O] complex. The interaction between adsorbed VOC molecules and this complex result in conversion of organic compound to CO_2 and water.

To study the competition for adsorption on the surface and also, as industrial waste gas streams commonly contain a mixture of several VOCs, we followed the oxidation of a mixture of toluene and propene. Fig. 8 presents the conversion of each component (toluene and propene) separately and of simple mixtures in the presence of Pd(shell)–Au(core)/TiO_2 catalyst. A comparison between T_{50} (temperature for 50% of conversion) of toluene and propene oxidation reaction shows that propene oxidizes at lower temperature than

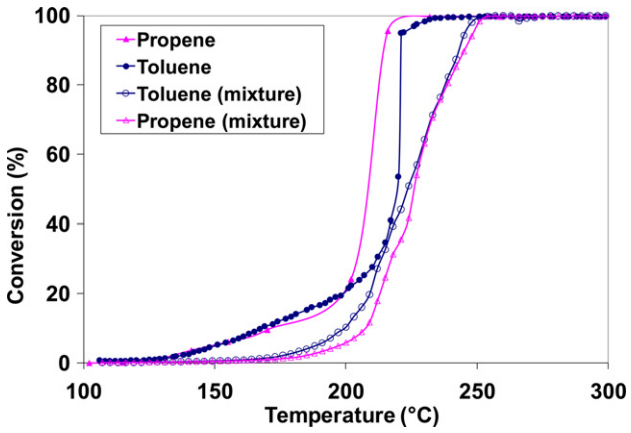

Fig. 8. Conversion of toluene and propene separately and in the mixture on Pd(shell)–Au(core)/TiO_2.

toluene. In the mixture, the T_{50} corresponding to the propene oxidation increases by 15 °C while these temperatures for toluene are close. It was observed that the presence of toluene modifies the catalytic activity of this catalyst for oxidation of propene, where the presence of propene has no significant effect on toluene oxidation. The results revealed then, the existence of a mixture effect in the form of inhibition of the oxidation of propene in the presence of toluene. Such inhibiting effects could be attributed to competitive adsorption of the VOCs molecules on the surface of catalyst.

It is known that the oxidation of a VOC in a mixture generally differs from its single oxidation due to the interaction of the different species with the catalyst [52]. Ordenez et al. [53] also shown that hexane oxidized at lower temperature than those of benzene and toluene, but in a mixture, benzene and toluene inhibit the oxidation of hexane. This phenomenon was explained by the preferential adsorption of toluene and benzene on the surface of the catalyst. In the case of our catalyst, it seems also that there is a preferential adsorption of toluene on the surface of catalyst and the oxidation of propene does not happen until the toluene is not converted.

In order to understand the competition for adsorption of toluene and propene molecules on the catalyst, the catalytic performance was also followed by Operand DRIFT under the same conditions as the normal test. Fig. 9 shows the IR spectra obtained in the presence of catalyst Pd(shell)–Au(core)/TiO_2 and a mixture of toluene and propene at 100, 150, 200, 260, 310, 350 and 400 °C. The results have shown the decrease and disappearance of some bands and also the appearance of new bands corresponding to the formation of intermediate compounds during the oxidation reaction. The adsorptions observed at 1644, 1510 and 1420 cm^{-1} correspond to the vibration of aromatic C=C of toluene adsorbed on the surface of catalyst.

The band at 1644 cm^{-1} decreases after 150 °C and then disappears at 260 °C by total conversion of toluene. In addition, the intensity of the bands at 1510 and 1420 cm^{-1} increases after 150 °C until 310 °C and then decrease. The variation of the intensity could correspond to the formation of substituted aromatics and then combustion of these compounds between 300 and 400 °C. This kind of variation has been observed in the toluene test (spectra not shown) while in the case of propene these byproducts form simultaneously [20]. The difference could be explained by the fact that the formed hydrocarbon residues during propene conversion tend to resist oxidation. The band at 1589 cm^{-1} that presents a maximum at 200 °C and then a decrease, could be attributed to the vibration of C=C bond of aromatic cycle. This band that was not observed for the oxidation of propene, forms during the oxidation of the mixture and disappears at high temperatures. The same evaluation of this band was observed for the oxidation of toluene. The temperature of T_{50} obtained by the oxidation test and the results

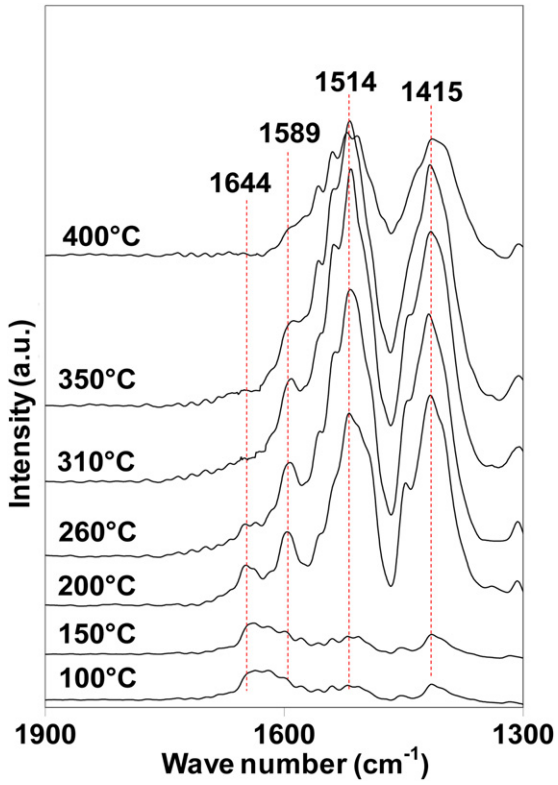

Fig. 9. Operando DRIFT spectra of mixture of toluene and propene on Pd(shell)–Au(core)/TiO_2.

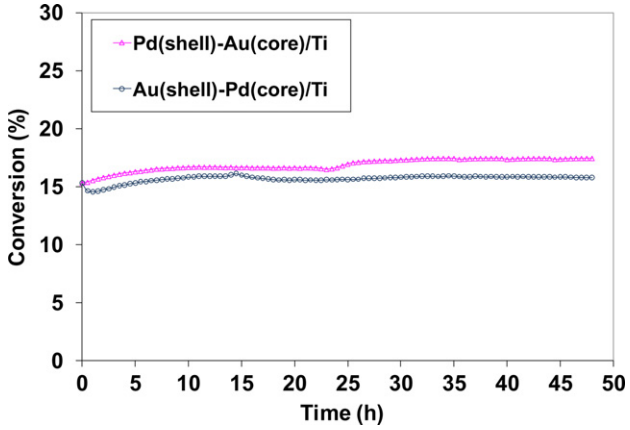

Fig. 10. Long-term activity test for Pd(shell)–Au(core) and Au(shell)–Pd(core)/TiO_2.

obtained by the spectra of Operando DRIFT during the test of mixture have confirmed the previously adsorption of toluene compared to propene.

Since the formation of intermediate compounds was observed by Operando DRIFT and DTA-TGA analysis [26], it is interesting to analyze the behavior of the catalysts for a long-term application. The used catalysts were tested under toluene flow at a temperature corresponding to 15% of reaction for 50 h. The results (Fig. 10) show that the catalysts are active and stable during the test. As a result, formation and deposition of unwanted reaction products do not appear to have an effect on the efficiency and activity of catalyst.

4. Conclusion

This work investigates the preparation and activity of Pd(shell)–Au(core)/TiO_2, Au(shell)–Pd(core)/TiO_2 and Pd–Au(alloy)/TiO_2 catalysts for the total oxidation of VOC. The catalysts Pd(shell)–Au(core) and Au(shell)–Pd(core)/TiO_2 have been synthesized by different order of deposition of metal. The sample Pd–Au(alloy)/TiO_2 was prepared by depositing Pd and Au at the same time. The higher activity of Pd(shell)–Au(core)/TiO_2 was obtained for toluene and propene oxidation compared to those of Au(shell)–Pd(core) and Pd–Au(alloy). The UV–vis and XPS spectra and also TPR profiles confirmed the presence of core–shell morphology for the particles of gold and palladium. The results obtained by characterization and catalytic test allow to better understand the mechanism of oxidation reaction in the presence of toluene and propene. It has been suggested that the mechanism of oxidation reaction proceeds through the preferential adsorption of oxygen molecules on the surface of catalysts where there is a competition for adsorption between the molecules of oxygen and VOC. The difference of catalytic activity observed for these catalysts could be related to their core–shell and alloy morphology. It was found that catalytic activity is significantly higher with Pd–shell and Au-core morphology. Moreover, the lower activity of Au(shell)–Pd(core)/TiO_2 could also be correlated to its lower affinity for adsorption of oxygen due to the lower ability of Au to polarize oxygen molecule.

The catalytic test in the presence of gases streams containing mixtures of toluene and propene molecules has shown that in the mixture propene oxidize at a higher temperature compared to those of separated. We evidenced by Operando DRIFT that not only the inhibition effect of toluene for oxidation of propene but also the competition for adsorption between toluene and propene molecules. Moreover, because the formation of unwanted products was observed by operando DRIFT, the used catalysts have been tested under toluene flow. The catalysts were found stable and active after 50 h.

Acknowledgements

The authors thank IRENI and the European community through an Interreg IIIa and IV (Redugaz) France-Wallonie-Flandre projects and Walloon Region for financial supports.

References

[1] R.K. Sharma, B. Zhou, S. Tong, K.T. Chuang, Ind. Eng. Chem. Res. 34 (1995) 4310.
[2] A.C. Gluhoi, N. Bogdanchikova, B.E. Nieuwenhuys, Catal. Today 113 (2006) 178.
[3] M.D. Robbins, M.A. Henderson, J. Catal. 238 (2006) 111.
[4] J.J. Spivey, Ind. Eng. Chem. Res. 26 (1987) 2165.
[5] C. Gennequin, M. Lamallem, R. Cousin, S. Siffert, F. Aïssi, A. Aboukaïs, Catal. Today 122 (2007) 301.
[6] R. Gopinath, N. Lingaiah, N.S. Babu, I. Suryanarayana, P.S. Sai Prasad, A. Obuchi, J. Mol. Catal. A: Chem. 223 (2004) 289.
[7] S. Minico, S. Scirè, C. Crisafulli, R. Maggiore, S. Galvagno, Appl. Catal. B: Environ. 28 (2000) 245.
[8] J. Hong, C. Wei, M. Chen, X. Wang, T. Zhang, Catal. Commun. 8 (2007) 593.
[9] M.A.C. Nascimento, Theoretical Aspects of Heterogeneous Catalysis, vol. 8, Kluwer Academic Publishers, Dordrecht/Boston, MA, 2001.
[10] C. Kan, W. Cai, C. Li, L. Zhang, H. Hofmeister, J. Phys. D: Appl. Phys. 36 (2003) 1609.
[11] Y. Mizukoshi, K. Okitsu, Y. Maeda, T.A. Yamamoto, R. Oshima, Y. Nagata, J. Phys. Chem. B 101 (1997) 7033.
[12] S. Marx, A. Baiker, J. Phys. Chem. C 113 (2009) 6191.
[13] D. Wang, A. Villa, F. Porta, L. Prati, D. Su, J. Phys. Chem. C 112 (23) (2008) 8617.
[14] Y.W. Lee, N.H. Kim, K.Y. Lee, K. Kwon, M. Kim, S.W. Han, J. Phys. Chem. C 112 (17) (2008) 6717.
[15] D. Jana, A. Dandapat, G. De, J. Phys. Chem. C 113 (21) (2009) 9101.
[16] R.W.J. Scott, O.M. Wilson, S.-K. Oh, E.A. Kenik, R.M. Crooks, J. Am. Chem. Soc. 126 (47) (2004) 15583.
[17] A.A. Herzing, A.F. Carley, J.K. Edwards, G.J. Hutchings, C.J. Kiely, Chem. Mater. 20 (2008) 1492.
[18] H. Falsig, B. Hvolbaek, I.S. Kristensen, T. Jiang, T. Bligaard, C.H. Christensen, J.K. Angew Norskov, Chem. Int. Ed. 47 (2008) 4835.
[19] I.N. Remediakis, N. Lopez, J.K. Norskov, Appl. Catal. A 291 (2005) 13.
[20] M. Hosseini, S. Siffert, H.L. Tidahy, R. Cousin, J.-F. Lamonier, A. Aboukaïs, A. Vantomme, B.-L. Su, Catal. Today 122 (2007) 391.

[21] W.-J. Shen, M. Okumura, Y. Matsumura, M. Haruta, Appl. Catal. A: Gen. 213 (2001) 225.
[22] B. Xie, Y. Xiong, R. Chen, J. Chen, P. Cai, Catal. Commun. 6 (2005) 699.
[23] X. Lai, T.P. St. Clair, M. Valden, D.W. Goodman, Prog. Surf. Sci. 59 (1998) 25.
[24] F. Sun, S. Zhong, J. Nat. Gaz. Chem. 15 (2006) 45.
[25] M.P. Kapoor, Y. Ichihashi, K. Kuraoka, Y. Matsumura, J. Mol. Catal. A: Chem. 198 (2003) 303.
[26] M. Hosseini, S. Siffert, R. Cousin, A. Aboukaïs, Z. Hadj-Sadok, B.-L. Su, C. R. Chim. 12 (2009) 654.
[27] M. Haruta, S. Tsubota, T. Kobayashi, H. Kegeyama, M.J. Genet, B. Delmon, J. Catal. 144 (1993) 175.
[28] J. Graham, Hutchings, Catal. Today 138 (2008) 9.
[29] J.K. Edwards, B.E. Solsona, P. Landon, A.F. Carley, A. Herzing, C.J. Kiely, G.J. Hutchings, J. Catal. 236 (2005) 69.
[30] D.I. Enache, D. Barker, J.K. Edwards, S.H. Taylor, D.W. Knight, A.F. Carley, G.J. Hutchings, Catal. Today 122 (2007) 407.
[31] D.I. Enache, J.K. Edwards, P. Landon, B. Solsona-Espriu, A.F. Carley, A.A. Herzing, M. Watanabe, C.J. Kiely, D.W. Knight, G.J. Hutchings, Science 311 (2006) 362.
[32] A. Abad, P. Concepcion, A. Corma, H. Garcia, Angew. Chem., Int. Ed. 44 (2005) 4066.
[33] K. Mori, T. Hara, T. Mizugaki, K. Ebitani, K. Kaneda, J. Am. Chem. Soc. 26 (2004) 10657.
[34] A. Corma, M.E. Domine, Chem. Commun. (2005) 4042.
[35] H. Takatani, F. Hori, M. Nakanishi, R. Oshima, Aust. J. Chem. 53 (2003) 1025.
[36] H. Takatani, H. Kago, Y. Kobayashi, F. Hori, R. Oshima, Trans. Mater. Res. Soc. Jpn. 28 (2003) 871.
[37] V. Idakiev, L. Iilieva, D. Andreeva, J.-L. Gigot, B.-L. Su, Appl. Catal. A: Gen. 243 (2003) 25.
[38] M. Cozzolino, M. Di Serio, R. Tesser, E. Santacesaria, Appl. Catal. A: Gen. 325 (2007) 256.
[39] H. Nur, Mater. Sci. Eng. B 133 (2006) 49.
[40] J.-E. Park, T. Momma, T. Osaka, Electrochim. Acta 52 (2007) 5914.
[41] K. Esumi, M. Nawa, N. Aihara, K. Usui, New J. Chem. (1998) 719.
[42] M.B. Mohamedi, K.Z. Ismail, S. Link, M.A. El-Sayed, J. Phys. Chem. B 102 (1998) 9370.
[43] B.M.I.V.D. Zande, M.R. Böhmor, L.G.J. Fokkink, C. Schönenberger, J. Phys. Chem. B 101 (1997) 852.
[44] Y. Li, Y. Fan, H. Ynag, B. Xu, L. Feng, M. Yang, Y. Chen, Chem. Phys. Lett. 372 (2003) 160.
[45] S. Devarajan, P. Bera, S. Sampath, J. Colloid Interf. Sci. 290 (2005) 117.
[46] D. Dalucu, J.E. Klemberg-Sapieha, L. Martinu, Surf. Sci. 472 (2001) 33.
[47] A.M. Venezia, V. La Parola, G. Deganello, B. Pawelec, J.L.G. Fierro, J. Catal. 215 (2003) 317.
[48] W.R. MacDonald, K.E. Hayes, J. Catal. 18 (1970) 115.
[49] N.V. Kul'kova, L.L. Levchenko, Kin. Katal. 6 (1965) 688.
[50] H. Berndt, I. Pitsch, S. Evert, K. Struve, M.-M. Pohl, J. Radnik, A. Martin, Appl. Catal. A: Gen. 224 (2003) 169.
[51] M.N. Huda, A.K. Raya, Eur. Phys. J. B 43 (2005) 131.
[52] T. Garcia, B. Solsona, D.M. Murphy, K.L. Antcliff, S.H. Taylor, J. Catal. 229 (2005) 1.
[53] S. Ordenez, L. Bello, H. Sastre, R. Rosal, F.V. Diez, Appl. Catal. B: Environ. 38 (2002) 139.